Revealing Local Dynamics of the Protonic Conductor $CsH(PO_3H)$ by Solid-State NMR Spectroscopy and First-Principles Calculations

Gunwoo Kim,[1,2] John M. Griffin,[1,†] Frédéric Blanc,[1,2,#] David M. Halat,[1] Sossina M. Haile[3] and Clare P. Grey[1,2]*

[1] Department of Chemistry, University of Cambridge,

Lensfield Road, Cambridge, CB2 1EW, United Kingdom,

[2] Department of Chemistry, Stony Brook University,

Stony Brook, NY 11790-3400, United States,

[3] Department of Materials Science and Engineering, Northwestern University

Evanston, IL 60208, United States.

Present address: [†] Department of Chemistry, Lancaster University,

Lancaster, LA1 4YB, United Kingdom,

[#] Department of Chemistry, University of Liverpool,

Stephenson Institute for Renewable Energy, Liverpool, L69 7ZD, United Kingdom.

* Author to whom correspondence should be addressed (C.P.G.):

Email: cpg27@cam.ac.uk; Phone: +44 (0)1223 336509; Fax: +44 (0)1223 336509.

Abstract

A joint study incorporating multinuclear solid-state NMR spectroscopy and first-principles calculations has been performed to investigate the local structure and dynamics of the protonic conductor $CsH(PO_3H)$ in the paraelectric phase. The existence of the superprotonic phase (>137 ºC) is clearly confirmed by NMR, in good agreement with the literature. The variable-temperature ^{1}H, ^{2}H and ^{31}P NMR data further reveal a distribution of motional correlation times, isotropic rotation of the phosphite ion being observed below the superprotonic phase transition for a small but gradually increasing subset of anions. This isotropic rotation is associated with fast local protonic motion, the distribution of correlation times being tentatively assigned to internal defects or surface absorbed H_2O. The phosphite ion dynamics of the majority slower subset of phosphite ions is quantified through analysis of variable-temperature ^{17}O spectra recorded from 34 to 150 ºC, by considering a model for the pseudo C_3 rotation of the phosphite ion around the P-H bond axis below the phase transformation. An extracted activation energy of 0.24 ± 0.08 eV (23 ± 8 kJ mol^{-1}) for this model was obtained, much lower than that reported from proton conductivity measurements, implying that no strong correlation exists between long range protonic motion and C_3 rotations of the phosphite. We conclude that proton conduction in $CsH(PO_3H)$ in the paraelectric phase is governed by both the activation energy for exchange between donor and acceptor oxygen sites, rotation of the phosphite units, and the lack of isotropic rotation of the phosphite ion. Surprisingly, coalescence of ^{17}O NMR resonances, as would be expected for rapid isotropic reorientations of all phosphite groups, is not observed above the transition. Potential reasons for this are discussed.

1. Introduction

Fuel cells that function in the intermediate temperature range of 200 – 600 ºC have been widely recognized as important technologies in a sustainable energy future because of their potential for efficient conversion of chemical to electrical energy under conditions that circumvent the need for costly auxiliary components.[1-3] Achieving fuel cell operation under such conditions requires the availability of appropriate electrolytes. Cesium dihydrogen phosphate (CsH_2PO_4 or CDP) with a proton conductivity of ~2×10^{-2} $S \cdot cm^{-1}$ at 233 °C[4] is attractive in this regards, and substantial technological progess in CDP-based fuel cells has been made in recent years.[5] Nevertheless, development of electrolytes with even more favorable characteristics would provide advantages, an outcome that can result from a fundamental understanding of the origins of high protonic conductivity in CDP and related materials. Like CDP, the compound $CsH(PO_3H)$ (cesium hydrogen phosphite or CHP) is a solid acid compound and displays an analogous transition to a high temperature, high conductivity crystalline phase with extreme structural disorder. Study of the phosphite polyanion, with its favorable characteristics for nuclear magnetic resonance (NMR) spectroscopy, creates an opportunity to understand the origins of high protonic conductivity in this important class of materials. With this objective in mind, we use a combined experimental and first-principles NMR study of CHP, using both static and magic angle spinning (MAS) methods, to examine the local structure and dynamics of this material upon transition from the paraelectric phase (that adopted under ambient conditions) into the high temperature phase. The proton and anion dynamics are compared to our earlier results for CDP.[6,7]

2 Background

At room temperature, CHP crystallizes in a monoclinic phase[8] of space group $P2_1/c$. This structure, Figure 1, has two crystallographically distinct cesium atoms and two hydrogen phosphite ions ($HPHO_3^-$). Each atom of the structure resides on a general position, resulting in eight molecular units per unit cell ($Z = 8$). The tetrahedral corners of the phosphite groups are defined by one hydrogen atom, forming a direct P-H bond, and three oxygen atoms. Of the oxygen atoms, two are involved in hydrogen bonds, with one serving as the donor in such a bond and one serving as an acceptor. Thus, each vertex is chemically distinct. The P-H bond in the phosphite is presumably much more covalent than the P-O bonds. Moreover, whereas in CDP ionic charges of P^{5+}, O^{2-} and H^+ result in a charge balanced formula, in CHP one can either consider the P to be P^{3+} forming a direct bond with H^+, or to be P^{5+} forming a direct bond with H^-. This chemical difference can be expected to give rise to difference in the NMR chemical shifts relative to CDP. The two crystallographic types of phosphite groups in CHP are linked in the structure in alternating fashion via the hydrogen bonds, forming chains described according to $[P1\text{-}O3\text{-}H2\cdots O5\text{-}P2\text{-}O6\text{-}H4\cdots O2]_n$, where O3 and O6 are the donors and O2 and O5 are the acceptors.[8] Hereafter the H2 and H4 atoms are referred to as the acidic protons, and the H1 and H3 species directly bonded to P atoms are termed protons without reference to their actual (unknown) oxidation states.

Although both the structure and chemistry of CHP and CDP differ significantly at room temperature, both compounds adopt the CsCl structure type at high temperature with the pseudo tetrahedral polyanion group disordered over six possible orientations, a surprising configuration for the phosphite unit given its lower symmetry.[9-11] The transformation to the cubic phase, known as a superprotonic transition as a result of the accompanying increase in conductivity by several orders of magnitude, occurs at 137 ºC in CHP,[9,12] somewhat lower than the transition temperature

of 228 °C in CDP.[13] The conductivity of superprotonic CHP is somewhat lower (3×10^{-3} S·cm^{-1} at 160 °C[12]) than that of CDP (1.8×10^{-2} S·cm^{-1} at 233 °C[4]), a feature attributed, in part, to the lower polyanion symmetry.[8]

3 Experimental methods

3.1 Sample preparation and characterization CHP was synthesized from a stoichiometric aqueous mixture of starting materials, H_3PO_3 and Cs_2CO_3, using a slow evaporation method described previously[9]. Isotopically-enriched CHP samples (of target formulae $CsD(PO_3D)$ and $CsH(P^{17}O_3H)$) were prepared by dissolving $CsH(PO_3H)$ (120 mg, 0.561 mmol) into either D_2O (2 g, 100 mmol, 99% Aldrich) or ^{17}O-enriched H_2O (0.286 g, 15.1 mmol, 20.9% Cortecnet) and then the solution was dried under vacuum at 100 ºC for 2 - 3 days. The extent of deuteration and ^{17}O-enrichment resulting from this treatment was not quantified, but based on NMR signal intensities, was found to be relatively small. The compound CHP is hygroscopic and therefore all pristine and isotopically-enriched compounds were stored and packed into rotors for the NMR experiments in dry argon atmosphere to minimize the contact with humidity. Formation of the target phase was confirmed in all cases by PXRD, Figure S1 (Panalytical Empyrean X-ray diffractometer, Cu Kα radiation), with no impact from the isotopic enrichment.

3.2 NMR All magic angle spinning (MAS) NMR spectra for ^1H, ^2H, ^{31}P and ^{17}O were obtained using a Hahn-echo pulse sequence (unless otherwise stated) on a 16.4 T Bruker Avance III 700 NMR spectrometer equipped with a 1.3 mm HX (for ^1H, and ^{31}P), and a 4 mm HXY (for ^1H, ^2H, and ^{17}O) MAS probe heads, respectively. High resolution room temperature spectra for ^1H and ^{31}P were collected using a MAS frequency of 60 kHz and a recycle delay of 200 - 500 s. Variable-temperature ^1H NMR experiments were carried out using a MAS frequency of 12.5 kHz (and a recycle delay of 400 s).

For ^{2}H, for which room and variable-temperature MAS spectra were collected under identical spectrometer conditions, RF power was set to 50 kHz and the spectra were acquired by a single-pulse experiment with a MAS frequency of 12.5 kHz and a recycle delay of 10 s. In addition, ^{1}H decoupling was applied to suppress linebroadening due to dipolar interaction between deuterons and residual protons. For the variable-temperature ^{2}H experiments, the magic angle was carefully adjusted in a separate experiment for each temperature by minimizing the linewidth of the OD resonance of d_4-malonic acid. The experiment was then repeated with the CHP sample at the same temperature. Due to thermal decomposition of malonic acid >135 ºC, it was not possible to adjust the magic angle at higher temperatures (>120 ºC) with this standard, and thus there are likely to be small deviations in the magic angle at higher temperatures.

Room and variable-temperature MAS spectra were both collected for ^{17}O employing a double frequency sweep (DFS) scheme so as to enhance the signal to noise ratio[14,15] and compensate for incomplete ^{17}O-enrichment. Optimized parameters for the DFS were determined using ^{17}O-enriched CsH_2PO_4 as a reference compound. Specifically, the ^{17}O RF pulse power was set to 50 kHz and the recycle delay to 1 s, with a MAS frequency of 12.5 kHz.

Variable-temperature ^{31}P NMR spectra were acquired under static conditions on an 8.45 T Varian Chemagnetics Infinity Plus 360 MHz spectrometer using a 4 mm HX MAS Chemagnetics probehead. ^{1}H and ^{31}P RF pulse strengths were set to 83 – 100 kHz and, for cases in which decoupled spectra were desired, a ^{1}H decoupling power of 60 – 100 kHz was used.

The sample temperature in both spectrometers was calibrated, with an accuracy of ± 5 °C, using the ^{207}Pb resonance of $Pb(NO_3)_2$ in a separate MAS experiment.[16,17] Somewhat larger errors in the quoted temperatures are expected for the VT ^{31}P static NMR experiments, because the

temperature calibration has been made under MAS conditions, the difference between sample and measured temperature depending strongly on bearing and driving gas pressures under MAS.

Chemical shifts of ^{1}H, ^{2}H, ^{31}P, and ^{17}O were externally referenced to H_2O at 4.8 ppm, D_2O at 4.8 ppm, 85% H_3PO_4 at 0 ppm, and H_2O at 0 ppm, respectively. Unless otherwise specified, fitted and simulated NMR spectra were generated using DMFit and SIMPSON, respectively.[18,19] The influence of oxygen exchange was evaluated using the EXPRESS 3.0[20] program. Similar to our previous ^{17}O NMR study of CsH_2PO_4,[7] a simple three-site exchange model was assumed to simulate the effect of the phosphite ion rotation on the ^{17}O NMR line shapes. Simulations of the ^{31}P chemical shift anisotropy (CSA) were carried out with DMFit.[19]

3.3 First-principles calculations First-principles calculations of NMR parameters were carried out using the CASTEP version 6 density functional theory (DFT) code,[21] in combination with the GIPAW algorithm,[22] which allows the reconstruction of the all-electron wave function in the presence of a magnetic field. The generalized gradient approximation (GGA) PBE functional[23] was employed, and core-valence interactions were described by ultrasoft pseudopotentials.[24,25] Calculations were performed using a planewave energy cut-off of 60 Ry (816 eV) and integrals over the Brillouin zone were obtained using a *k*-point spacing of 0.04 $Å^{-1}$. The calculations generate the absolute shielding tensor ($\boldsymbol{\sigma}$) in the crystal frame. Diagonalization of the symmetric part of $\boldsymbol{\sigma}$ yields the three principal components, σ_{XX}, σ_{YY} and σ_{ZZ}. The isotropic shielding, σ_{iso}, is given by $(1/3)\mathrm{Tr}\{\boldsymbol{\sigma}\}$. The isotropic chemical shift, δ_{iso}, is given by $-(\sigma_{iso} - \sigma_{ref})$, where σ_{ref} is the reference shielding value. For ^{17}O ^{31}P, and ^{1}H, respective reference shieldings of 268, 280, and 30.5 ppm were used.[7,26-28] The quadrupolar coupling constant, $C_Q = eQV_{ZZ}/h$, and electric-field gradient (EFG) asymmetry parameter, $\eta_Q = (V_{XX} - V_{YY})/V_{ZZ}$, are obtained directly from the principal components of the electric field gradient tensor, which are ordered such that $|V_{ZZ}| \geq$

$|V_{YY}| \geq |V_{XX}|$, where Q is the nuclear quadrupole moment of ^{2}H and ^{17}O (2.9×10^{-31} and -25.6×10^{-31} m^2, respectively[29]). Prior to calculation of the NMR parameters, the experimentally-determined structure was geometry-optimized using a cut-off energy of 50 Ry (680 eV) and *k*-point spacing of 0.04 $Å^{-1}$. Unit cell parameters and atomic coordinates were allowed to freely vary; the approximate symmetry of the final structure was found to be consistent with the $P2_1/c$ space group of the original crystallographic arrangement.

4 Results

4.1 Insight into the room-temperature structure of $CsH(PO_3H)$ The room-temperature ^{1}H NMR spectrum of CHP under ultra-fast MAS conditions shown in Figure 2a reveals two well-resolved proton environments: OH (an acidic proton), with an isotropic shift of 10.4 ppm, and PH (a proton directly bound to phosphorus), with an isotropic shift of 7.0 ppm. The PH proton resonances appear as two overlapping doublets due to P-H scalar *J*-coupling with a single chemical shift value of 7.0 ppm and a $^{1}J_{P\text{-}H}$ coupling constant of ~ 620 Hz. The latter is in reasonable agreement with the P-H coupling constant of 752 Hz reported for H_3PO_3.[30] The isotropic resonances for the pairs of protons in the two distinct phosphite units are unresolved, both in the measurement and in the simulation, highlighting their close structural similarity. Indeed, the calculated shift values, Table S1, indicate that there is only 0.1 ppm difference in H1 *vs*. H3 and H2 *vs*. H4 shifts. This difference is smaller than the line broadening caused by the proton homonuclear dipolar interaction, which is difficult to completely remove, even by fast MAS.

The features of the ^{2}H NMR spectrum of deuterated CHP, Figure S2, are similar to those of the ^{1}H spectrum, with distinct resonances evident for the OD and PD environments at 10.4 and 7.2 ppm, respectively. The associated quadrupolar coupling constants, C_Q, Table S1, are 164 and

106 kHz, respectively, in good agreement with the calculated pairs of values of {164, 160} and {109, 110}, respectively. The calculated shifts for both ^{1}H and ^{2}H resonances are larger than those observed experimentally, especially for the protons/deuterium ions directly bound to oxygen atoms, which are also larger than one would predict based on the reported correlation between shift and hydrogen bond length.[31,32] Using instead a known correlation between the experimental ^{2}H C_Q and ^{1}H chemical shift[33], a value of 10.2 ppm is predicted for the ^{1}H resonance, in excellent agreement with the experimental data, perhaps taking into account the OH/OD motions in the system. We note that planewave DFT calculations have a known tendency to overestimate the chemical shift of hydrogen-bonded OH protons, thought to be at least partly related to the fact that finite temperature effects are not accounted for.[34]

Similar to the ^{1}H spectrum, the room-temperature ^{31}P NMR spectrum, again under ultra-fast MAS conditions, (Figure 2b) reveals a doublet due to scalar *J*-coupling between ^{31}P and ^{1}H nuclei. As with the ^{1}H and ^{2}H spectra, the two crystallographically-distinct phosphorus sites P1 and P2 are not resolved. The coupling constant extracted from the lone doublet at δ_{iso} = -6.7 ppm of $^{1}J_{P\text{-}H}$= ~ 610 Hz is in good agreement with the value obtained from the ^{1}H NMR data. The calculations predict experimental resolution between the ^{31}P chemical shifts of the P1 and P2 species. Specifically, the calculated positions (see Table S2) are -5.7 and -7.2 ppm, respectively (a frequency separation of ~ 430 Hz at 16.4 T), whereas the linewidth of the ^{31}P resonances is only 0.7 ppm ($\Delta\nu_{½}$ = ~ 200 Hz). Experimental coalescence of these peaks is tentatively attributed to averaging effects due to small motions at room temperature, which the 0 K calculation does not treat.

The ^{31}P static NMR spectrum collected with ^{1}H decoupling is dominated by the resonance at δ_{iso} = -6.7 ppm (Figure 2c; also see further details in Table S2). Using a single ^{31}P CSA

component fit a chemical shift anisotropy (δ_{aniso}) of -101 ppm is extracted, substantially smaller than the calculated values of -122 and -120 ppm for P1 and P2, respectively. A similar deviation has been reported in a previous study of phenylphosphinic acid $C_6H_5HPO(OH)$,[35] and has been attributed to local motion in the near vicinity of the P-H bond at room temperature. While smaller than the DFT calculated value, the experimental ^{31}P CSA for CHP with its asymmetric local bonding environment about phosphorous is, as expected, significantly larger than that found in CDP (-46 ppm at 8.45 T[6]), which has close to tetrahedral symmetry about P (*i.e.,* PO_3H *vs*. PO_4). While the single-component model provided a reasonable fit to the data (Fig. 2(c)(i)), a noticeable improvement is obtained when an additional sharper resonance (free of CSA broadening) is included with a fraction of 7 % (Fig. 2(c)(ii)). This feature is discussed below in the context of the variable-temperature measurements.

The ^{17}O DFS MAS NMR spectrum of CHP (Figure 2d) exhibits a broad signal made up of a number of partially resolved second-order quadrupolar-broadened resonances. Three different oxygen sites are distinguished, but again, the analogous environments between different crystallographically-distinct phosphite units (*i.e.* O3/O6, O2/O5, and O1/O4) are indistinguishable, consistent with the calculations also presented in the figure. On the basis of the simulations, the resonance at the lowest frequency (with a center of gravity of approximately 80 ppm) is assigned to the donor oxygen atoms in the H-bonds (O3 and O6), and the shifts of the acceptor oxygen atoms (O2 and O5) are at approximately 110 ppm. The highest-frequency resonance (at around 150 ppm) is assigned to the P-O oxygen atoms (O1 and O4), which are neither proton donors nor acceptors. Beyond agreement of the relative peak positions with the simulations, the experimental spectrum shows fairly good agreement in peak breadths and line shapes with the simulated results. In CDP a similar trend of ^{17}O shift values was observed, with

the resonances of the donor oxygen atoms being located at a frequency lower by about 50 ppm than those of the acceptors. However, the ^{17}O shift values in CHP are substantially higher than those in CDP, for example by 40 ppm in the case of the donor oxygen atoms.[7] This difference is likely a result of differences between the electronic structures of the PO_3H and PO_4 anions, which in turn, affect the chemical shielding of each oxygen site.[35]

The experimental spectrum has been fit to extract the NMR parameters, as summarized in Table S3. The DFT-calculated ^{17}O C_Q values are slightly larger than those obtained from experiment, but a similar trend for overestimation of C_Q values was observed in the calculated NMR parameters of CDP.[7] Furthermore, the magnitude of the C_Q values for each oxygen site follows a trend of the reported C_Q values from different local oxygen environments in a similar phosphite-containing system, where the ^{17}O C_Q values for oxygen forming P-<u>O</u>H bonds are larger than those forming P=<u>O</u> bonds.[35] However, the fits to the O3/O6 site were poor, resulting in large errors for the C_Q and η_Q values for this species. The poor fit obtained with a single set of ^{17}O NMR parameters for this site, (Figure 2d), may be due to either a motional process, a spectral distortion due to the use of a DFS enhancement resulting in non-uniform excitation, or the presence of different local environments due to defects and/or slightly different quadrupolar parameters/chemical shifts for the two crystallographic O3/O6 sites.

In sum, the room-temperature NMR spectra are generally consistent with the DFT computed spectra based on the geometry optimized 0 K structure. Significantly, the analogous chemical environments within the two similar, but crystallographically-distinct, phosphite units in the crystal structure are not experimentally resolved. The calculations indicate that the resonances are either so close in frequency that they overlapped (^{1}H and ^{17}O), or suggest that the sites cannot be distinguished due to motional effects (^{31}P).

4.2 Proton dynamics: variable-temperature ^{1}H and ^{2}H NMR Figure 3 shows the variable-temperature ^{1}H MAS spectra of CHP in the range 34 – 150 ºC, with details of the spectral features provided in Table S4. Substantial changes with temperature are evident. The PH proton resonance slightly sharpens, but its features are otherwise generally unchanged by heating up to 134 °C. The resonance corresponding to the acidic H-bonded (10.6 ppm) proton also narrows over this temperature range ($\Delta\nu_{½}$ = ~ 320 and ~ 50 Hz at 77 and 134 ºC, respectively) and additionally gradually decreases in intensity. Most striking is the emergence at 77 ºC of a resonance at a high frequency of 13.4 ppm, which intensifies, sharpens and shifts to lower frequency upon approaching the phase transition. On the basis of the sharpness of this resonance and the absence of associated spinning sidebands, its origin is tentatively assigned to the presence of a highly mobile proton species. At 150 ± 5 °C, the resonance associated with the acidic proton of the monoclinic structure disappears and is completely replaced by the higher frequency resonance. Simultaneously, the *J*-coupled doublet also becomes very sharp ($\Delta\nu_{½}$ = ~ 140 Hz at 150 ºC).

This set of changes in the ^{1}H MAS spectra is largely a reflection of the monoclinic to cubic transition. The phase transition is found to occur here between 134 and 150 °C, in good agreement with the reported transition temperature (130 – 150 °C).[9] The observation of a narrow resonance at 12.2 ppm ($\Delta\nu_{½}$ = ~ 30 Hz at 150 ºC) in the high temperature phase is consistent with the presence of fast diffusive motion of protons in the superprotonic state of CDP[6]. The sharpness of the *J*-coupled doublet at 150 ºC moreover indicates rapid reorientation of the P-H bond and the reduction of broadening due to homonuclear dipolar coupling. The changes to the spectra at temperatures below the transition are, in contrast, unexpected. The emergence of a sharp resonance at high frequency due to mobile protons, coexisting alongside the resonance of

the acidic proton, suggests the presence of a distribution of proton dynamics in the paraelectric phase.

Variable-temperature ^{2}H MAS NMR spectra (see Figure S3 and Table S5) exhibit similar features. At 34 °C two resonances, due to the OH and PH protons (the latter a doublet due to scalar coupling), are evident. On heating, a high frequency resonance emerges, first detectable at 115 °C, at a resonance of ~ 12.5 ppm. Small changes in the ^{2}H spinning sideband manifolds are also observed from 115 °C, consistent with the onset of motion. The position of the emergent high frequency peak due to mobile species gradually shifts from ~ 12.5 ppm at 115 °C to 11.8 ppm at 141 °C, while the peak furthermore sharpens and grows substantially. In parallel, the intensity of the acidic proton peak diminishes. The coexistence of acidic proton and highly mobile proton peaks again suggests the presence of a distribution of proton dynamics in the paraelectric phase. The protonic (deuteron) motion is evidently too slow to affect the ^{2}H line shape (≃ 100 kHz) and therefore only qualitatively establishes an upper limit of protonic motion in the paraelectric phase of CHP.

4.3 Anion dynamics in the paraelectric phase: variable-temperature ^{31}P and ^{17}O NMR The variable-temperature ^{31}P static NMR spectra and extracted parameters are presented in Figure 4 and Table S6, respectively. With ^{1}H decoupling, Figure 4a, the spectra exhibit a composite line shape composed of a broad pattern arising from the CSA and a sharper resonance described by a Gaussian/Lorentzian line shape, as shown in (ii) of Figure 2c. The same features are observed across the whole temperature range of the paraelectric phase. Upon heating, the span of the ^{31}P CSA remains unchanged (as observed in our previous study of CDP[6]), but the intensity of this CSA-broadened component gradually decreases. Simultaneously, the sharp resonance gradually increases in intensity and shifts from 5.2 to -1.8 ppm in the temperature range 25 – 130 ºC. At

140 ºC, only this narrow resonance is observed (δ_{iso} = -1.7 ppm; $\Delta\nu_{1/2}$ = 1.2 kHz). We ascribe this feature to the fast reorientation of the phosphite ion in the superprotonic phase. The loss of intensity from the CSA-broadened component between 130 and 140 ºC implies a phase transition temperature lying within this temperature range, consistent with that observed by ^{1}H and ^{2}H MAS NMR spectroscopy (a transition temperature between 135 and 150 ºC).

The variable-temperature ^{31}P spectra obtained without ^{1}H decoupling are shown in Figure 4b. The room-temperature line shape is dominated by ^{31}P CSA and ^{1}H-^{31}P dipolar interactions, including the strong dipolar coupling of the P-H pair (d = ~ 20 kHz). As the temperature is increased, the spectrum changes and, similar to the results obtained with decoupling (Figure 4a), a sharp resonance emerges. The motion that gives rise to this new resonance clearly results in the removal of both the CSA and ^{1}H-^{31}P dipolar coupling, as evidenced by the appearance of this sharp peak both with and without proton decoupling.

These changes in the ^{31}P line shape in the paraelectric phase of CHP indicate a significant distribution of phosphite motional rates, consistent with the distribution of correlation times for proton motion in the ^{1}H NMR spectra (Figure 3). The CSA-broadened rigid component (Figure 4b) must result from coordination of the phosphorous by a set of anions (three oxygen atoms and one hydrogen atom) that do not undergo isotropic motion on the order of, or faster than, the NMR timescale probed in this experiment, which is in this case, the size of the ^{31}P CSA (~15 kHz at 8.45 T). Three-fold rotation about the P-H bond is possible, but rotation about the P-O bonds is not, because this would result in an exchange between P-O and P-H bonds; such motion would induce a reduction in ^{1}H-^{31}P dipolar coupling and thus line narrowing. In contrast, the narrower (Gaussian/Lorentzian) resonance in the paraelectric phase is tentatively attributed to phosphite ion rotation about all four P-X bonds of the tetrahedral ion, given its similarity to the

resonance observed in the superprotonic phase (Table S6). Furthermore, isotropic reorientation of the phosphite group can account for a reduction in the ^{1}H-^{31}P dipolar coupling as observed. At room temperature the sharp resonance, observed with a relative fraction of 7 % (Figure 2c), is noticeably broader ($\Delta\nu_{1/2}$ = 3.4 kHz) and more shifted to higher frequency than that detected at higher temperatures. Therefore, it is unclear whether the motional processes that give rise to the sharp resonance at ambient temperature are the same as those giving rise to this feature at higher temperatures.

The behavior of CHP found here contrasts that of CDP. In our previous NMR study we observed a single lineshape in the ^{31}P spectrum of this phosphate system, which displayed a decrease in ^{1}H-^{31}P dipolar coupling effects upon heating, ascribed to proton dynamics, but minimal change in the CSA. We were further able to isolate phosphate ion C_3 rotations about the P-OH bond (occurring at high rate) from other types of rotations (occurring at lower rate).[7] Because protons are not directly bonded to phosphorous in CDP, a fixed CSA in that compound is compatible with even isotropic tetrahedral reorientations of the phosphate group.

As with the variable-temperature ^{1}H, ^{2}H, and ^{31}P spectra, the variable-temperature ^{17}O DFS MAS NMR spectra of CHP displayed significant changes with temperature, Figure 5a, particularly above 134 ºC. Upon heating, the sharp spectral features associated with the second-order quadrupolar line shapes become gradually broadened for all oxygen sites, indicating the onset of motion; however, coalescence of these peaks (*i.e.,* in the slow motional regime) is not observed at any temperature across the range studied. Instead, the peaks corresponding to the three oxygen sites remain distinct. This implies that the phosphite reorientation in CHP is restricted, even in the superprotonic phase. Importantly, broadening of the O1/O4 resonance (at approximately 150 ppm), is noticeable at the higher temperatures and comparable to that of the

other oxygen resonances, indicating that this non-H-bonded oxygen is also involved in the observed motional process in CHP.

NMR lineshape simulations have been carried out in an effort to uncover the nature of the motional process. Because the broadening indicates participation in the motion by all oxygen atoms, a model in which the phosphite group rotates about the P-H bond axis (*i.e.*, a pseudo C_3 (3-fold) rotation), resulting in hops between oxygen sites with a rate constant k_{ex}, has been considered (Figure S4). The simulated line shapes, Figure 5b, show satisfactory agreement with the ^{17}O experimental data, indicating the validity of this model. At 134 ºC (the highest temperature recorded for the paraelectric phase) an oxygen exchange rate constant of 1 kHz is obtained. An Arrhenius plot of the rate constant (Figure 5c) shows a linear relationship over the temperature range 77 – 134 ºC (entirely within in the paraelectric phase), with an activation energy (E_a) of 0.24 ± 0.08 eV (23 ± 8 kJmol^{-1}). A sharp jump in the rate occurs at 150 ºC, consistent with the overall rapid dynamics in the superprotonic phase.

5. Discussion and Conclusions

First-principles calculations have enabled the interpretation of the different chemical environments in ^{1}H, ^{2}H, ^{31}P, and ^{17}O NMR spectra of CHP at room temperature, showing reasonable agreement between computed and measured chemical shifts. Variable-temperature ^{1}H, ^{2}H, and ^{31}P NMR experiments clearly reveal that the superprotonic phase transition takes place at ~140 °C. The broad resonances evident in the ^{1}H, ^{2}H and ^{31}P NMR spectra of the paraelectric phase abruptly disappear at this temperature. On heating from ambient temperature, the spectra furthermore show the gradual appearance of sharp isotropic resonances, which then fully describe the spectra in the high temperature phase. The absence of spinning sidebands in both ^{1}H and ^{2}H data indicates the presence of fast proton dynamics in this phase, whereas sharp

isotropic resonances, as observed in the high temperature ^{1}H, ^{2}H, and ^{31}P NMR spectra, generally reflect rapid isotropic motion in solids.

A distinguishing feature of the ^{1}H, ^{2}H, and ^{31}P NMR spectra is the gradual appearance of sharp resonances in the paraelectric phase of CHP, which emerge in conjunction with the dominant broad resonances of the ambient temperature spectra. In particular, an additional sharp component is evident in the room-temperature ^{31}P NMR line shape of CHP under static conditions. The coexistence of sharp and broad resonances, which has not been observed for CDP, indicates the presence of a distribution of motional correlation times in the paraelectric phase of CHP. The origin of this distribution is not clear, but is tentatively attributed to the presence of surface-sorbed water as a result of the strongly hygroscopic nature of the material. A recent NMR and conductivity study of LiH_2PO_4 has revealed that proton transport in this material largely arises from surface-sorbed H_2O, these protons undergoing dynamic exchange with protons in the bulk structure of the material.[36] Here, the more mobile protons at below the paraelectric phase transition may similarly result from exchange of bulk protons with residual/surface water, but may also be associated with defects within the sample. However, unlike the LiH_2PO_4 study, species associated with low levels of residual water in CHP were not detected by NMR.

In contrast to the ^{1}H, ^{2}H, and ^{31}P spectra, the ^{17}O NMR data for the paraelectric phase show evidence for restricted, rather than free, rotation of the phosphite groups, as coalescence of the three oxygen resonances from the three different classes of oxygen atoms is not observed even at 150 °C. Furthermore, there is no evidence in the data for a distribution of correlation times for motion (*i.e.,* we do not observe the more mobile components). It is possible that the ^{17}O spin-lattice relaxation time (T_1) in the superprotonic phase is significantly longer than in the

paraelectric phase and thus motional effects on the spectra are not observed due to saturation by the short experimental recycle delay of 1 s. Furthermore, the use of the DFS sequence during acquisition of the spectrum, which relies on population transfer from satellite transitions to the central transition, may play a role. A highly mobile component, which does not have satellite transitions, will not be enhanced by DFS as much as the other environments, and so these peaks will not benefit from this signal enhancement method. Thus, we tentatively suggest that the VT ^{17}O DFS spectra represent *only* the ^{17}O line shape change from a subset of phosphite anion motions, those with relatively long correlation times for motion. Consistent with this interpretation, a significant intensity loss of a factor of ~0.7 in the ^{17}O DFS spectrum at 150 ºC is observed compared to 77 ºC, which is more than the expected loss of ~0.2 due to a Boltzmann temperature factor. Although in principle, it would be possible to test this hypothesis by performing experiments at >150 ºC, doing so was practically limited due to possible thermal decomposition of CHP.

Although coalescence of the ^{17}O resonances is not observed at high temperature, thermal effects are clearly evident. A simple C_3 rotation model around the P-H bond axis has been chosen here to describe the oxygen dynamics because motional influence (broadening) of the three ^{17}O sites is observed for all three central transition peaks at high temperatures, which provides good agreement with the experimental spectra, particularly in the paraelectric phase. Moreover, rapid rotation about a P-O axis would result in averaging of the ^{31}P CSA (δ_{aniso} = -101 ppm, ~15 kHz at 8.45 T), since this rotation changes the orientation of the P-H vs. P-O bonds. The slow motion observed by ^{17}O spectroscopy (< 1kHz in the paraelectric phase) is consistent with the high resolution ^{1}H, ^{2}H, and ^{31}P spectra which only show one H/D-P, or P environment, respectively, rather than the two expected from crystallography suggesting that these spectra may be sensitive

to local motion that interconverts the different sites. The ^{1}H and ^{2}H spectra at 150 °C are sensitive to a different type of motion, that of highly mobile ions in the superprotonic phase. That no sidebands of the superprotonic feature are observed in these spectra shows that this rapid motion is roughly on the order of, or faster than, the MAS frequency (12.5 kHz), consistent with the sharp ^{31}P resonances seen at this temperature.

Dynamics in the paraelectric phases of CDP and CHP, as revealed by NMR spectroscopy, share some intriguing characteristics, but are also distinguished in others. A key difference between the two materials surrounds the nature of the tetrahedral group reorientations. In CHP, C_3 reorientations about the P-H bond are detected, but not about the P-O bonds; in addition, a subset of the phosphorus atoms (the fraction of which increases with temperature) are in an isotropic environment suggestive of isotropic rotation of the polyanion. In CDP, in which all oxygen atoms form hydrogen bonds, two types of rotations are detected, rotation about the P-O_d bond, where O_d represents the donor in a hydrogen bond, and rotation about the bonds to the other three ligands of the phosphate group, *i.e.*, rotations about P-O bonds in which the oxygen is effectively an acceptor in a hydrogen bond.

Despite this difference, both materials undergo reorientations of the tetrahedral group with apparently greater ease than they support long-range proton transport. In CHP reorientation about the P-H bond occurs with an activation energy of 0.24 ± 0.08 eV, as extracted from the estimated rotational frequency, which is substantially smaller than the activation energy of 0.74 ± 0.01 eV for long-range proton transport obtained from conductivity measurements in the temperature range 80 – 120 ºC.[9] In CDP, a mean activation energy for tetrahedral group reorientation of 0.43 ± 0.05 eV was extracted, again much smaller than the value of 0.91 ± 0.05 eV obtained from conductivity measurements.[37] For the phosphate, it was further possible to

directly measure proton exchange dynamics, from which an activation energy of 0.70 ± 0.07 eV was determined, and an exchange rate much smaller than the tetrahedral reorientation rate was also determined. Thus, in both materials, tetrahedral group reorientation in the paraelectric phase is apparently decoupled from long-range protonic motion.

In a further similarity, the activation energy for rotation about P-O_d in CDP, 0.21 ± 0.06 eV, is comparable to that for rotation about P-H in CHP (0.24 ± 0.08 eV) in their respective paraelectric phases. This, combined with the apparent decoupling of such rotations from long-range proton transport, loosely suggests that the reorientations in both cases occur without redistribution of proton positions in the structure. That is, the oxygen site exchange that occurs upon rotation about the P-H or P-O_d axes may do so without any accompanying proton motion. In such case, hydrogen bonds would be locally broken during reorientation and reformed in the same arrangement subsequent to the reorientation. The alternative, in which the proton remains attached to an oxygen atom as the latter moves into a new oxygen site (*e.g.*, O3 and its accompanying proton moving to site O2 in CHP, Figure 1), would require not only that the hydrogen bond be broken during reorientation, but also the formation of hydrogen bond defects upon conclusion of the motion,[38] likely requiring a high activation energy.

Finally, two characteristics appear in CHP that do not appear in CDP. The first is rapid proton motion in a subset of the protonic species occurring at temperatures substantially below the superprotonic transition. This has been tentatively attributed to either water adsorbed on the surface of the CHP particles or other defects within the sample. However, again, we stress that we do not have any direct experimental evidence to support the presence of surface adsorbed water, other than the well-established hygroscopic nature of this material. The second is slow oxygen dynamics in the superprotonic phase, as evidenced by the retention of unique resonances

for the three ligands of the phosphite group. While this effect may be exaggerated as a result of the DFS enhancement method, experimental artifacts cannot explain the origin of this effect. Instead, we suggest that the asymmetry of the phosphite group retards the tetrahedral reorientation relative to that observed in CDP.

Acknowledgments

G.K., F.B., and C.P.G. thank the NSF *via* grant DMR0804737, and the New York State Foundation for Science, Technology and Innovation *via* a NYSTAR award. C.P.G. and G.K. thank the European Research Council for an Advanced Fellowship. F.B. thanks the EU Marie Curie actions FP7 for an International Incoming fellowship (grant *no* 275212) for financial support. J.M.G. also thanks the European Research Council for funding. G.K. thanks Dr. Michal Leskes for fruitful discussions about ^{17}O DFS experiments, Dr. Riza Dervişoğlu for valuable discussions about DFT calculations.

Supporting Information Available

PXRD (Figure S1), room-temperature ^{2}H MAS NMR spectra (Figure S2), summarized ^{2}H, ^{31}P, and ^{17}O NMR parameters at RT (Table S1, S2, and S3), summarized VT ^{1}H, ^{2}H, and ^{31}P NMR parameters (Table S4, S5, S6 and Figure S3), additional simulations of ^{17}O spectra (Figure S4), and illustration of proton exchange correlated with phosphite rotations (Figure S5). This material is available free of charge on the Internet at http://pubs.acs.org.

References

(1) Wachsman, E. D.; Lee, K. T. Lowering the Temperature of Solid Oxide Fuel Cells. *Science* **2011**, *334*, 935-939.

(2) Norby, T. Solid-State Protonic Conductors: Principles, Properties, Progress and Prospects. *Solid State Ionics* **1999**, *125*, 1-11.

(3) Fuel Cell Today. http://www.fuelcelltoday.com/media/1889744/fct_review_2013.pdf (accessed Aug 15, 2017).

(4) Haile, S. M.; Chisholm, C. R. I.; Sasaki, K.; Boysen, D. A.; Uda, T. Solid Acid Proton Conductors: from Laboratory Curiosities to Fuel Cell Electrolytes. *Faraday Discuss.* **2007**, *134*, 17-39.

(5) Chisholm, C. R. I.; Boysen, D. A.; Papandrew, A. B.; Zecevic, S. K.; Cha, S.; Sasaki, K. A.; Varga, Á.; Giapis, K. P.; Haile, S. M. From Laboratory Breakthrough to Technological Realization: The Development Path for Solid Acid Fuel Cells. *Electrochem. Soc. Interface* **2009**, *18*, 53-59.

(6) Kim, G.; Blanc, F.; Hu, Y.-Y.; Grey, C. P. Understanding the Conduction Mechanism of the Protonic Conductor CsH_2PO_4 by Solid-State NMR Spectroscopy. *J. Phys. Chem. C* **2013**, *117*, 6504-6515.

(7) Kim, G.; Griffin, J. M.; Blanc, F.; Haile, S. M.; Grey, C. P. Characterization of the Dynamics in the Protonic Conductor CsH_2PO_4 by ^{17}O Solid-State NMR Spectroscopy and First-Principles Calculations: Correlating Phosphate and Protonic Motion. *J. Am. Chem. Soc.* **2015**, *137*, 3867-3876.

(8) Kosterina, E. V.; Troyanov, S. I.; Kemnitz, E.; Aslanov, L. A. Synthesis and Crystal Structure of Acid Phosphites RbH_2PO_3, CsH_2PO_3, and TlH_2PO_3. *Russ. J. Coord. Chem.* **2001**, *27*, 458-462.

(9) Chisholm, C. R. I.; Merle, R. B.; Boysen, D. A.; Haile, S. M. Superprotonic Phase Transition in $CsH(PO_3H)$. *Chem. Mater.* **2002**, *14*, 3889-3893.

(10) Yamada, K.; Sagara, T.; Yamane, Y.; Ohki, H.; Okuda, T. Superprotonic Conductor CsH_2PO_4 Studied by ^{1}H, ^{31}P NMR and X-ray Diffraction. *Solid State Ionics* **2004**, *175*, 557-562.

(11) Preisinger, A.; Mereiter, K.; Bronowska, W. The Phase Transition of CsH_2PO_4 (CDP) at 505 K. *Mater. Sci. Forum* **1994**, *166*, 511-516.

(12) Zhou, W.; Bondarenko, A.; Boukamp, B.; Bouwmeester, H. Superprotonic Conductivity in $MH(PO_3H)$ ($M=Li^+, Na^+, K^+, Rb^+, Cs^+, NH_4^+$). *Solid State Ionics* **2008**, *179*, 380-384.

(13) Ikeda, A.; Haile, S. M. The Thermodynamics and Kinetics of the Dehydration of CsH_2PO_4 Studied in the Presence of SiO_2. *Solid State Ionics* **2012**, *213*, 63-71.

(14) Iuga, D.; Schäfer, H.; Verhagen, R.; Kentgens, A. P. M. Population and Coherence Transfer Induced by Double Frequency Sweeps in Half-Integer Quadrupolar Spin Systems. *J. Magn. Reson.* **2000**, *147*, 192-209.

(15) Iuga, D.; Kentgens, A. P. M. Influencing the Satellite Transitions of Half-Integer Quadrupolar Nuclei for the Enhancement of Magic Angle Spinning Spectra. *J. Magn. Reson.* **2002**, *158*, 65-72.

(16) Beckmann, P. A.; Dybowski, C. A Thermometer for Nonspinning Solid-State NMR Spectroscopy. *J. Magn. Reson.* **2000**, *146*, 379-380.

(17) Bielecki, A.; Burum, D. P. Temperature Dependence of ^{207}Pb MAS Spectra of Solid Lead Nitrate. An Accurate, Sensitive Thermometer for Variable-Temperature MAS. *J. Magn. Reson., Ser. A* **1995**, *116*, 215-220.

(18) Bak, M.; Rasmussen, J. T.; Nielsen, N. C. SIMPSON: A General Simulation Program for Solid-State NMR Spectroscopy. *J. Magn. Reson.* **2000**, *147*, 296-330.

(19) Massiot, D.; Fayon, F.; Capron, M.; King, I.; Le Calvé, S.; Alonso, B.; Durand, J.-O.; Bujoli, B.; Gan, Z.; Hoatson, G. Modelling One- and Two-dimensional Solid-State NMR Spectra. *Magn. Reson. Chem.* **2002**, *40*, 70-76.

(20) Vold, R. L.; Hoatson, G. L. Effects of Jump Dynamics on Solid State Nuclear Magnetic Resonance Line Shapes and Spin Relaxation Times. *J. Magn. Reson.* **2009**, *198*, 57-72.

(21) Clark, S. J.; Segall, M. D.; Pickard, C. J.; Hasnip, P. J.; Probert, M. J.; Refson, K.; Payne, M. C. First Principles Methods Using CASTEP. *Z. Kristallogr.* **2005**, *220*, 567-570.

(22) Pickard, C. J.; Mauri, F. All-electron Magnetic Response with Pseudopotentials: NMR Chemical Shifts. *Phys. Rev. B* **2001**, *63*, 245101.

(23) Perdew, J. P.; Burke, K.; Ernzerhof, M. Generalized Gradient Approximation Made Simple. *Phys. Rev. Lett.* **1996**, *77*, 3865-3868.

(24) Yates, J. R.; Pickard, C. J.; Mauri, F. Calculation of NMR Chemical Shifts for Extended Systems Using Ultrasoft Pseudopotentials. *Phys. Rev. B* **2007**, *76*, 024401.

(25) Vanderbilt, D. Soft Self-Consistent Pseudopotentials in a Generalized Eigenvalue Formalism. *Phys. Rev. B* **1990**, *41*, 7892-7895.

(26) Griffin, J. M.; Clark, L.; Seymour, V. R.; Aldous, D. W.; Dawson, D. M.; Iuga, D.; Morris, R. E.; Ashbrook, S. E. Ionothermal ^{17}O Enrichment of Oxides Using Microlitre Quantities of Labelled Water. *Chem. Sci.* **2012**, *3*, 2293-2300.

(27) Griffin, J. M.; Wimperis, S.; Berry, A. J.; Pickard, C. J.; Ashbrook, S. E. Solid-State ^{17}O NMR Spectroscopy of Hydrous Magnesium Silicates: Evidence for Proton Dynamics. *J. Phys. Chem. C* **2009**, *113*, 465-471.

(28) Griffin, J. M.; Berry, A. J.; Frost, D. J.; Wimperis, S.; Ashbrook, S. E. Water in the Earth's Mantle: A Solid-State NMR Study of Hydrous Wadsleyite. *Chem. Sci.* **2013**, *4*, 1523-1538.

(29) Pyykkö, P. Year-2008 Nuclear Quadrupole Moments. *Mol. Phys.* **2008**, *106*, 1965-1974.

(30) Schuster, M.; Kreuer, K. D.; Steininger, H.; Maier, J. Proton Conductivity and Diffusion Study of Molten Phosphonic Acid H_3PO_3. *Solid State Ionics* **2008**, *179*, 523-528.

(31) Eckert, H.; Yesinowski, J. P.; Silver, L. A.; Stolper, E. M. Water in Silicate Glasses: Quantitation and Structural Studies by Proton Solid Echo and Magic Angle Spinning NMR Methods. *J. Phys. Chem.* **1988**, *92*, 2055-2064.

(32) Yesinowski, J. P.; Eckert, H.; Rossman, G. R. Characterization of Hydrous Species in Minerals by High-Speed Proton MAS-NMR. *J. Am. Chem. Soc.* **1988**, *110*, 1367-1375.

(33) Sternberg, U.; Brunner, E. The Influence of Short-Range Geometry on the Chemical Shift of Protons in Hydrogen Bonds. *J. Magn. Reson., Ser. A* **1994**, *108*, 142-150.

(34) Webber, A. L.; Elena, B.; Griffin, J. M.; Yates, J. R.; Pham, T. N.; Mauri, F.; Pickard, C. J.; Gil, A. M.; Stein, R.; Lesage, A. et al. Complete ^{1}H Resonance Assignment of ß-maltose from ^{1}H-^{1}H DQ-SQ CRAMPS and ^{1}H (DQ-DUMBO)-^{13}C SQ Refocused INEPT 2D Solid-State NMR Spectra and First Principles GIPAW Calculations. *Phys. Chem. Chem. Phys.* **2010**, *12*, 6970-6983.

(35) Gervais, C.; Coelho, C.; Azaïs, T.; Maquet, J.; Laurent, G.; Pourpoint, F.; Bonhomme, C.; Florian, P.; Alonso, B.; Guerrero, G. et al. First Principles NMR Calculations of Phenylphosphinic Acid $C_6H_5HPO(OH)$: Assignments, Orientation of Tensors by Local Field Experiments and Effect of Molecular Motion. *J. Magn. Reson.* **2007**, *187*, 131-140.

(36) Kweon, J. J.; Fu, R.; Steven, E.; Lee, C. E.; Dalal, N. S. High Field MAS NMR and Conductivity Study of the Superionic Conductor LiH_2PO_4: Critical Role of Physisorbed Water in Its Protonic Conductivity. *J. Phys. Chem. C* **2014**, *118*, 13387-13393.

(37) Boyson, D. A.; Haile, S. M.; Liu, H.; Secco, R. A. High-Temperature Behavior of CsH_2PO_4 under Both Ambient and High Pressure Conditions. *Chem. Mater.* **2003**, *15*, 727-736.

(38) Bjerrum, N. Structure and Properties of Ice. *Science* **1952**, *115*, 385-390.

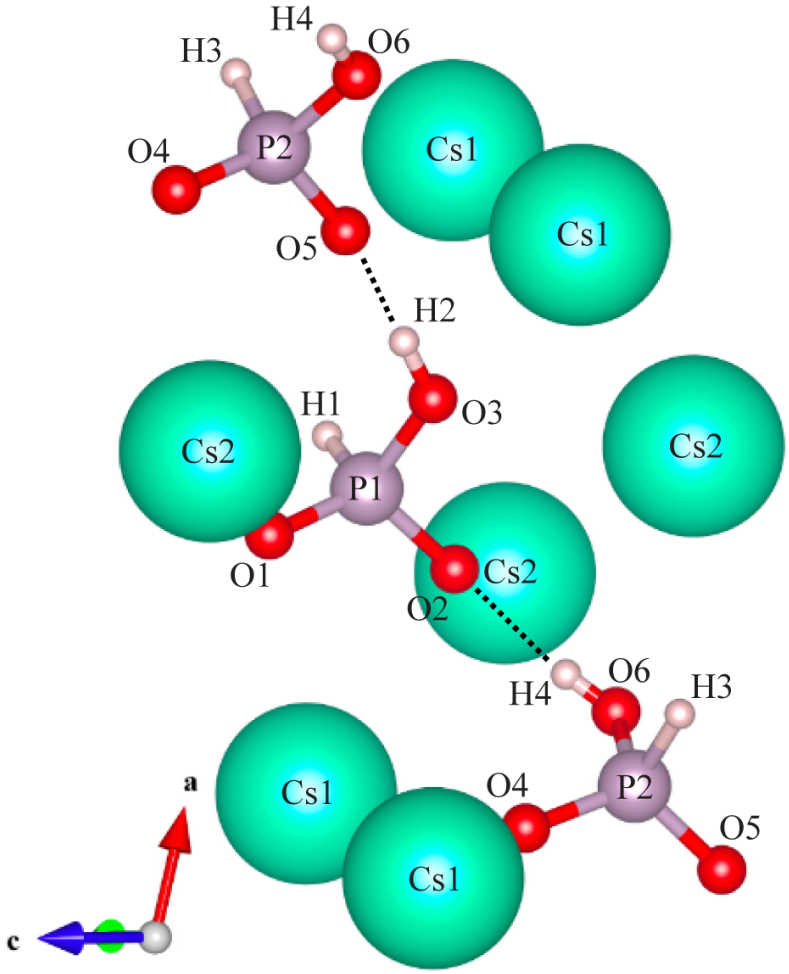

Figure 1. Crystal structure of $CsH(PO_3H)$ showing different crystallographic sites introduced by the two distinct phosphite ion orientations in the monoclinic phase with space group $P2_1/c$.[8] Atoms are labeled for clarity and hydrogen bonds are shown as dashed lines.

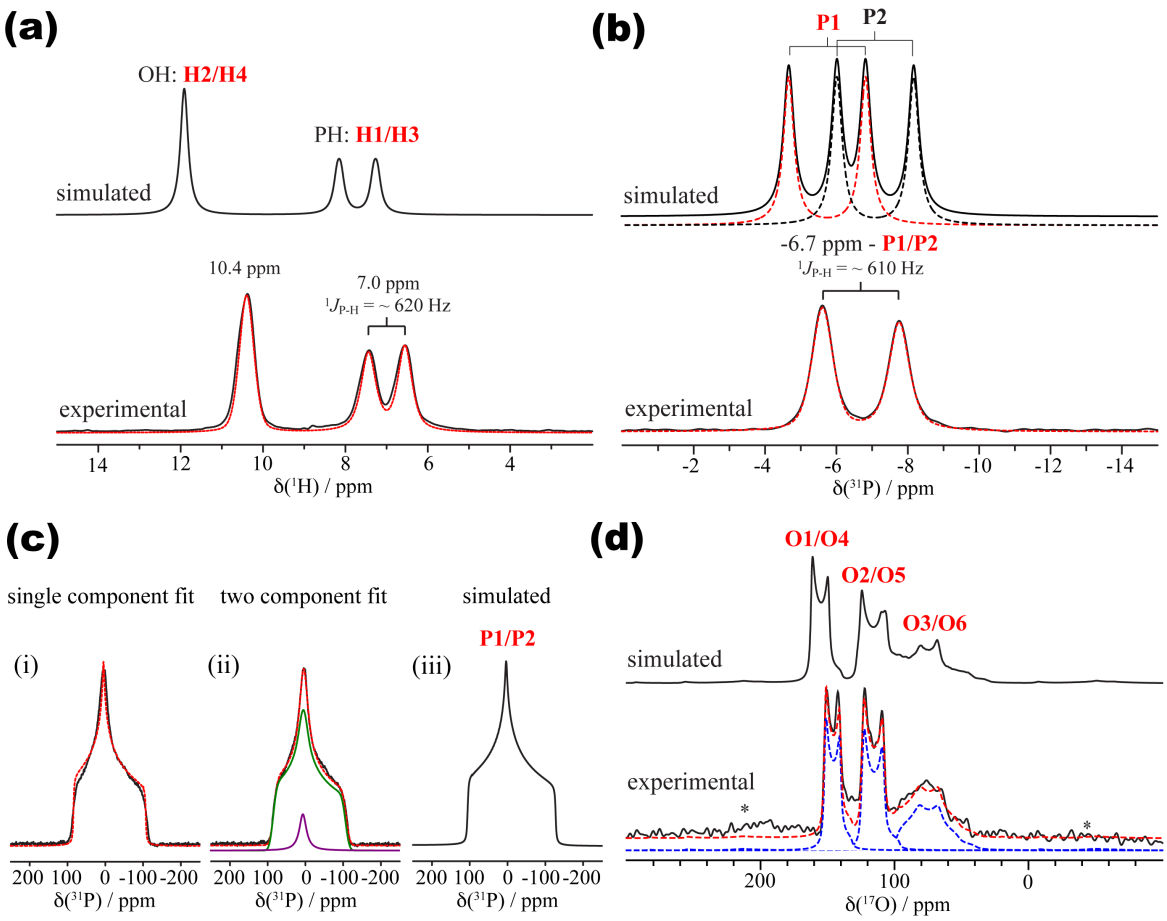

Figure 2. Multinuclear NMR spectra of $CsH(PO_3H)$ at room temperature: (a) ^{1}H, and (b) ^{31}P spectra acquired at 16.4 T with 60 kHz MAS, (c) ^{31}P spectra acquired at 8.45 T under static conditions with ^{1}H decoupling, showing static lineshapes and fits (red dashed lines) to the ^{31}P line shape assuming: (i) a single component fit assuming broadening by the ^{31}P CSA, and (ii) two component fit: a sharper resonance described by Gaussian/Lorentzian (purple solid line) and one broadened by the ^{31}P CSA (green solid line), and (iii) simulated spectrum using DFT calculated CSA parameters of P1 and P2 (with no attempt to account for an additional, sharp resonance), and (d) ^{17}O MAS DFS NMR spectra, acquired at 16.4 T with 12.5 kHz MAS. The corresponding crystallographic sites are labeled on the top of each spectrum and asterisks denote spinning sidebands. The total and individual fits are shown as red and blue dashed lines, respectively. The ^{17}O spectrum is simulated using the NMR parameters extracted from the DFT calculations (Table S3)

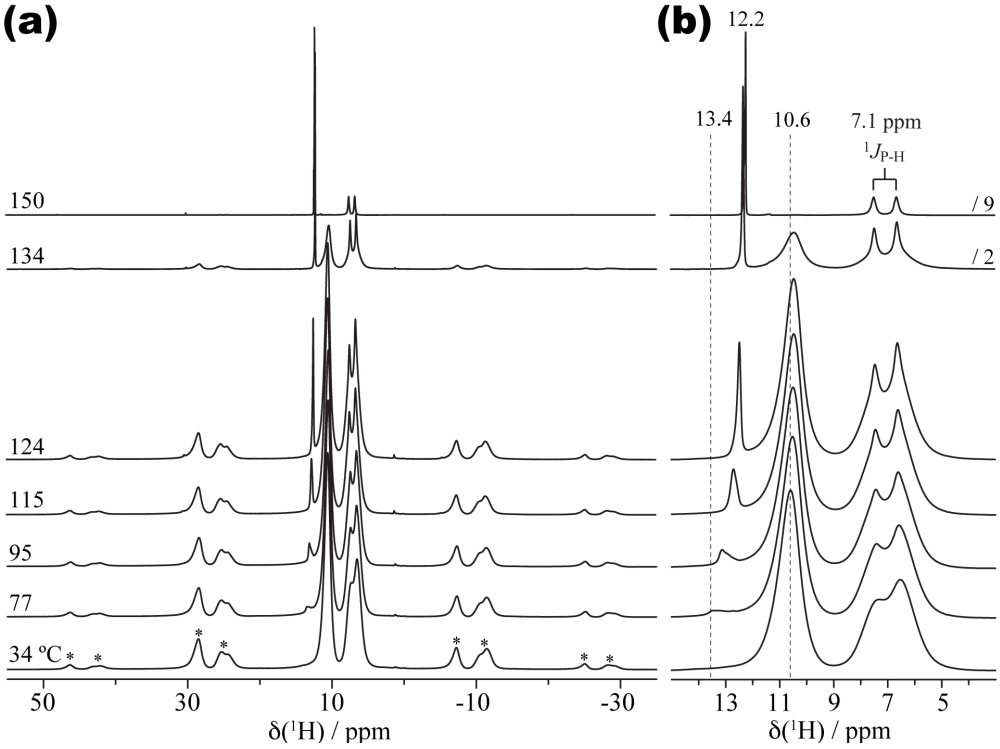

Figure 3. Variable-temperature ^{1}H MAS spectra of $CsH(PO_3H)$ acquired at 16.4 T at a MAS frequency of 12.5 kHz and recycle delay of 400 s, with (a) full spectral width showing the spinning sidebands (*), and (b) magnified isotropic region. The extracted isotropic shifts and corresponding intensities are summarized in Table S4.

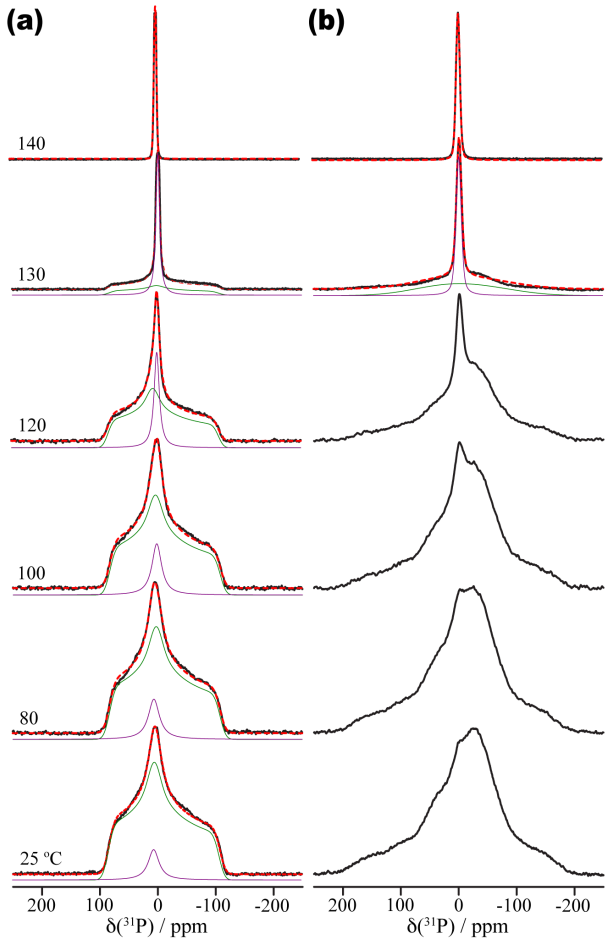

Figure 4. Variable-temperature ^{31}P static spectra of $CsH(PO_3H)$ (a) with and (b) without ^{1}H decoupling acquired at 8.45 T. The phase transition is observed at and above an apparent temperature of 130 ºC. The coexistence of signals from both the paraelectric and superprotonic phase at 130 ºC is ascribed to both a distribution of correlation times and a temperature gradient in the sample. Dashed lines show the best-fit simulations assuming two-component fit: a sharper resonance described by a Gaussian/Lorentzian and one broad line shape dominated by the ^{31}P CSA (purple and green traces, respectively). The extracted NMR parameters are summarized in Table S6.

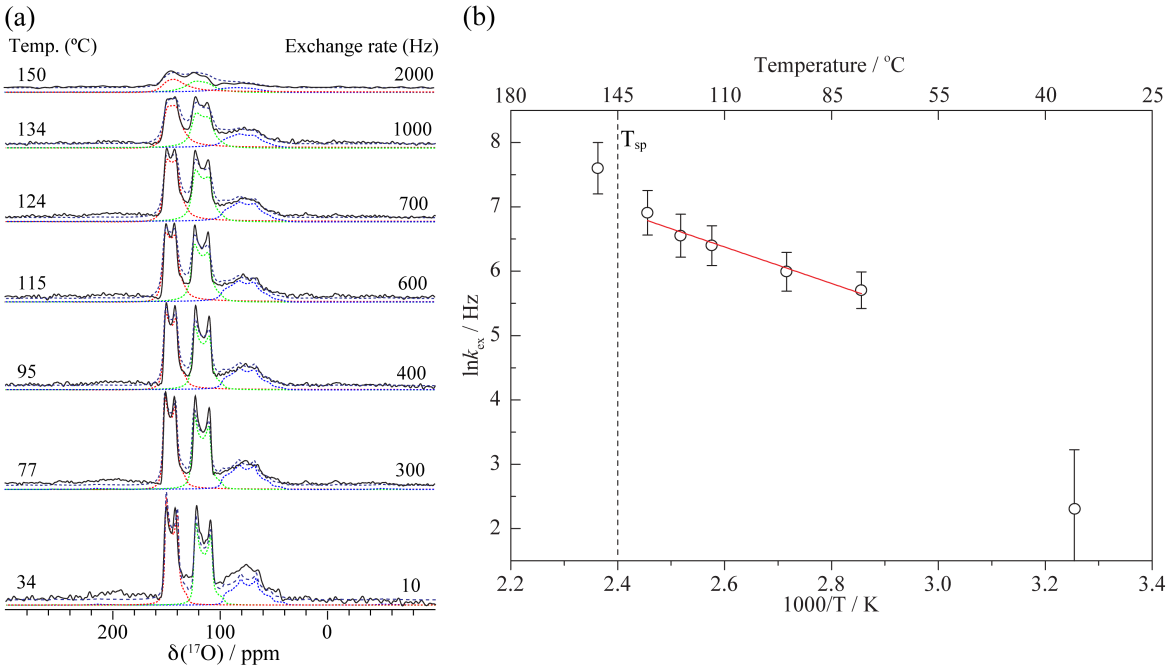

Figure 5. (a) Experimental ^{17}O DFS MAS NMR spectra (black traces) of $CsH(PO_3H)$ acquired at 16.4 T with a MAS frequency of 12.5 kHz as a function of temperature, with simulated ^{17}O line shapes (total fits as black dashed lines and the deconvolutions of the individual sites as red, green, and blue dotted lines) assuming an oxygen three-site exchange by a C_3 rotation around the P-H bond axis in the phosphite ion (PO_3H^{2-}) corresponding to an oxygen hop frequency k, and (b) Arrhenius plot of the ^{17}O three-site exchange rates (black open circles) obtained by NMR at 16.4 T, assuming C_3 rotation involving all oxygen sites. The red line corresponds to the least-square fit to the Arrhenius equation with $R^2 = 0.963$; error bars indicate errors of 5 % (40 % for the data point at room temperature). An activation energy of 0.24 ± 0.08 eV (23 ± 8 kJ mol^{-1}) is obtained from the fit in the 77 – 134 ºC temperature range.

TOC Graphic

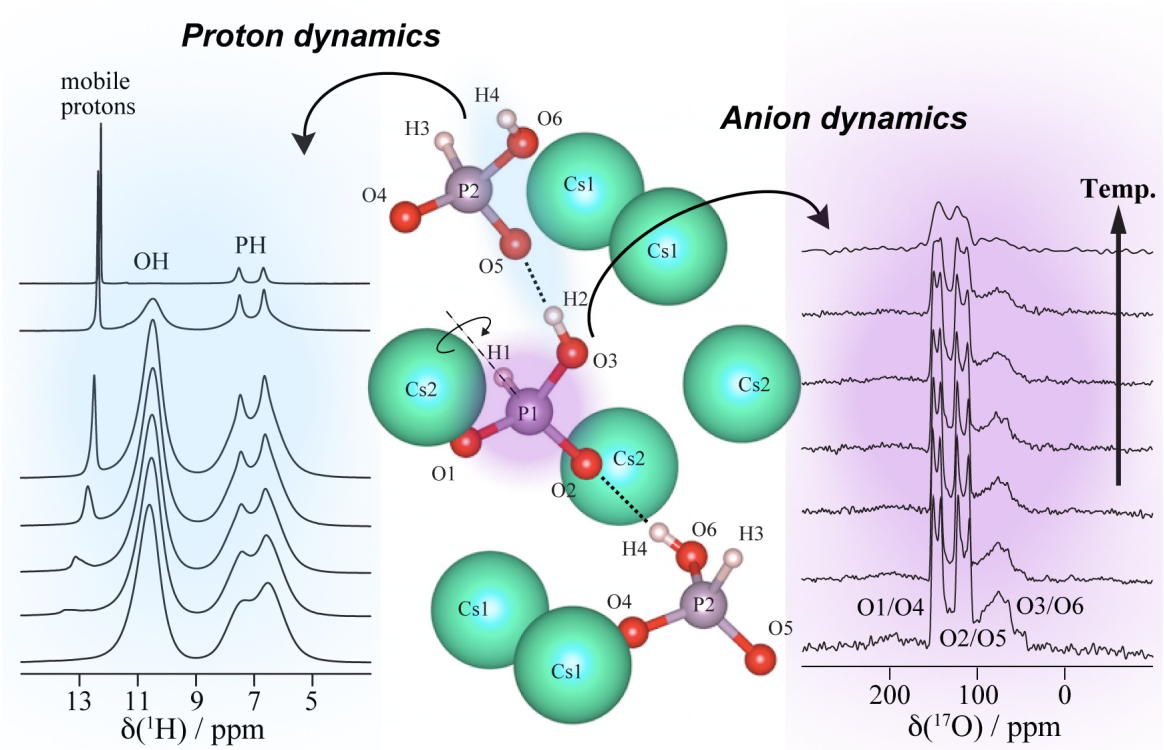
Proton dynamics
mobile protons
OH
PH
13
11
9
7
5
δ(1H) / ppm
H4
O6
H3
O4
P2
Cs1
Cs1
O5
H2
H1
O3
Cs2
P1
Cs2
Cs2
O1
O2
O6
H3
H4
Cs1
O4
P2
O5
Cs1
Anion dynamics
Temp.
O1/O4
O3/O6
O2/O5
200
100
0
δ(17O) / ppm